CRYSTAL GROWTH & DESIGN
2008
VOL. 8, NO. 7
2547–2554

Monotropic Polymorphism in Copper(II) Decanoate

M. Ramos Riesco,[†] F. J. Martínez Casado,[†] S. López-Andrés,[‡] M. V. García Pérez,[†] M. I. Redondo Yélamos,[†] M. R. Torres,[§] L. Garrido,[||] and J. A. Rodríguez Cheda*,[†]

Departamento de Química Física, Facultad de Ciencias Químicas, Universidad Complutense de Madrid, Spain, Departamento de Cristalografía y Mineralogia, Facultad de Ciencias Geológicas, Universidad Complutense de Madrid, Spain, CAI Difracción de Rayos X, Facultad de Ciencias Químicas, Universidad Complutense de Madrid, Spain, and Departamento de Química Física, Instituto de Ciencia y Tecnología de Polímeros, CSIC, Madrid, Spain

Received February 21, 2008; Revised Manuscript Received March 26, 2008

ABSTRACT: Copper(II) decanoate was synthesized, purified and studied by DSC, optical microscopy, XRD, and FTIR and C-13 NMR spectroscopies. Depending on the solvent used for crystallization two polymorphs were obtained. A combination of single-crystal and powder XRD was used to study their structures. One of the polymorphs (recrystallized in *n*-heptane) has similar structure to that previously reported at room temperature: triclinic (a = 7.94(1) Å, b = 5.28(3) Å, c = 28.13(5) Å; α = 94.6(10)°, β = 97.1(5)°, γ = 98.6(10)°). A single crystal of the second polymorph was obtained from an ethanol solution and has a triclinic structure (a = 5.2035(1) Å, b = 14.331(3) Å, c = 16.440(4) Å; α = 65.390(4)°, β = 86.889(4)°, γ = 82.886(4)°). This polymorph is monotropic and was identified by calorimetry as the metastable form. Both room temperature crystalline polymorphs belong to the same space group, $P\bar{1}$. However, they differ in (1) unit cell parameters; (2) one is bilayered whereas the other presents a columnar distribution of the binuclear complexes inside a net of two-by-two interdigitated chains. Thermal coefficients for both polymorphs have been estimated by indexation of their powder X-ray patterns versus temperature. The FTIR and C-13 NMR techniques confirm the structural differences. Both polymorphs melt to the same columnar discotic liquid crystal (identified by optical microscopy), decomposing before reaching the clearing point.

1. Introduction

Copper(II) alkanoates have been broadly studied during the last decades due to their potential as mesogens (form discotic liquid crystal phases) and also within the viewpoint of the coordination chemistry of copper.[1–4] This family has been studied by different techniques, including DTA[5] and DSC[1] calorimetries, FTIR[6,7] and Raman[6,8] vibrational and NMR[5] spectroscopies, dilatometry,[9] conductance,[10] or, to a great extent, by powder[1,4] and single crystal[11,12] X-ray diffraction. X-ray diffraction is undoubtedly the technique most used in the study of metal alkanoates in general, and in the copper(II) family in particular. The higher members of the copper(II), lead(II) and zinc alkanoates[13] (palmitates, oleates, stearates, linoleates) have been studied by X-ray diffraction. The interest in this group derives from their importance in the conservation of paintings or metal (lead, copper or zinc) artworks. They spontaneously appear inside the painting (reaction between pigments, as verdigris or white lead and zinc white, and organic acids generated from the oleo) or are used directly as thin films to protect metal artworks against aggressive environmental agents. This aspect gives to this series a further and striking interest.

Many reviews have discussed general aspects of the copper(II) alkanoate series, and those of Guiroud-Godquin's[14] (on metal containing liquid crystals) and Donnio[15] (on metallomesogens) are particularly relevant. Besides, Mrovzinski's[16] recent review on the molecular magnetism of copper alkanoates also highlights the suitability of this family of compounds for modeling electrical, magnetic and optical properties of materials.

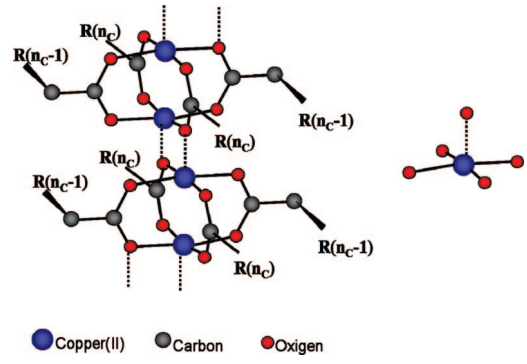

Figure 1. Two paddle wheel (molecular units) coordination. At the right, a CuO_4O chromophore group showing the copper square-pyramidal coordination.

The main structural feature of this family of compounds is that they exhibit a molecular unit (paddle-wheel) in the crystal structure (see Figure 1), thoroughly described by almost all of the cited authors. The Chinese lantern[17] complex was first used to describe this molecular unit and, more recently, paddle wheel,[18,19] which is more descriptive. This complex, which appears as a molecular unit in both the solid and fluid phases, is the reason why this family of compounds is not considered as an organic salt. This molecular unit receives in crystallography the names of tetrakis (μ-*o*-alkanoato) dicopper(II)[12] or catena-bis(μ_3-decanoato-*O*,*O*,*O*′)-bis(μ_2-decanoato-*O*-*O*′)-dicopper(II),[11b] instead of the more simple copper(II) decanoate. This unit consists in four triatomic O−C−O bridges coordinated to two copper(II) ions in an apical positions.

The coordination of copper is square-pyramidal,[15] forming CuO_4O chromophore groups (see Figure 1, right), in which the fifth oxygen atom belongs to the neighboring molecular unit (axial ligation), forming in this way a column or catena of molecular units coordinated to each other by two Cu−O bonds.

* Corresponding author. Tel: +34 91 3944306. Fax: +34 91 3944135. E-mail: cheda@quim.ucm.es.
[†] Departamento de Química Física, Facultad de Ciencias Químicas, Universidad Complutense de Madrid.
[‡] Departamento de Cristalografía y Mineralogia, Facultad de Ciencias Geológicas, Universidad Complutense de Madrid.
[§] CAI Difracción de Rayos X, Facultad de Ciencias Químicas, Universidad Complutense de Madrid.
[||] CSIC.

10.1021/cg800196s CCC: $40.75 © 2008 American Chemical Society
Published on Web 06/07/2008

In the already known room temperature crystal, these columns of axial coordinated units are organized parallel to each other to form a bilayered lamellar crystalline structure:[11b] lipidic layers of end chain CH_3 groups alternating with paddle-wheel layers. The catena are oriented in one direction of this layer, and the direct lateral packing of the molecular units takes place in the other one.

In the thermotropic mesophase, the internal structure of these columns of the complexes is retained, but the columns are organized according to a two-dimensional rectangular (copper(II) butanoate)[1c] or hexagonal[1] (all of the other members) lattice.

Another interest of these compounds is the formation of adducts.[18] Almost any kind of ligand donor of electron pairs (e.g., water,[20,21] organic acid,[22] urea,[19] pyridine-carboxylates,[23] etc.) is able to coordinate the copper(II) ions in the two apical positions of the paddle wheels. The pyridinecarboxylate[23] adducts attract great attention because of their medical interest. The therapeutic utility of copper complexes, with ligands having such properties, has been studied thoroughly.[24]

On the other hand, their simple synthesis has made copper(II) carboxylates interesting in materials science, as precursors in synthesis of metal−organic frameworks,[25] and as molecular templates in the synthesis of semiconductor nanorods, due to its self-assembling capacity over graphite substrates.[26] Another recent interest is the use of these compounds to get well dispersed copper nanoparticles by thermal decomposition in an inert atmosphere.[27,28]

Although the above cited references until here cover a period of more than 35 years, neither a polytype nor a monotropic polymorph has been reported elsewhere for any member of the whole copper(II) alkanoate series. Moreover, the monotropic polymorphism found in this work for copper decanoate adds a new interest to this compound. Polymorphs usually behave differently depending on a particular context. This case is particularly relevant in the pharmaceutical industry,[29] for which monotropic polymorphism may be considered of great practical and financial importance.[30]

Additionally, the copper(II) decanoate has been the less studied member of the series. For example, works on the even members of the whole series[1,8] lack the XRD *d*-spacings and DSC data for this compound. We attribute this lack of information to the complicated thermal behavior of this member of the copper(II) alkanoate series.

2. Experimental Section

2.1. Sample Preparation. For the synthesis of copper(II) decanoate, the choice can be open among a variety of different chemical reactions.[31] The adopted method was[11] the dropwise addition of decanoic acid (Fluka puriss. > 99.5%) to a hot suspension of basic copper(II) carbonate (Fluka purum p.a. > 95%) in excess, in absolute ethanol (Fluka puriss. > 99.8%), to which some milliliters of deionized water were also added. After 2−4 days, when evolution of CO_2 was no more apparent, the hot solution was filtered to remove the excess of carbonate. Then, the solvent was evaporated to reduce its volume to one-half and allowed to cool down to room temperature, and the flasks were kept at 273 K for 2−3 days, obtaining the first crystallization of the salt. The solids thus obtained were recrystallized at least three times from either *n*-heptane (Sigma, capillary GC, ≥99%) or benzene (Sigma, ACS reagent ≥99%), and finally dried under vacuum at about 383 K until constant weight. As it will be explained later, their behavior was different depending on the solvent used for recrystallization, corresponding to two different polymorphs. We will refer hereafter to sample (or polymorph) A for the one recrystallized in *n*-heptane, and sample (or polymorph) B for that recrystallized in benzene. Both samples were in the form of green-blue powders.

Table 1. Crystal Data and Structure Refinement for Polymorph B of $C_{40}H_{76}O_8Cu_2$

empirical formula	$C_{20}H_{38}CuO_4$
formula weight	406.04
temperature	296(2) K
wavelength	0.71073 Å
crystal system	triclinic
space group	$P\bar{1}$
unit cell dimensions	$a = 5.2035(11)$ Å $b = 14.331(3)$ Å $c = 16.440(4)$ Å $\alpha = 65.390(4)°$ $\beta = 86.889(4)°$ $\gamma = 82.886(4)°$
volume	1106.0(4) Å^3
Z	2
density (calculated)	1.219 Mg·m^{-3}
absorption coefficient	1.006 mm^{-1}
$F(000)$	438
crystal size	0.80 × 0.04 × 0.04 mm^3
index ranges	$-6 \le h \le 6$, $-18 \le k \le 18$, $-18 \le l \le 20$
reflections collected	9976
independent reflections	4754 [R(int) = 0.0672]
completeness to theta = 27.00°	98.3%
refinement method	full-matrix least-squares on F^2
data/restraints/parameters	4754/0/206
goodness-of-fit on F^2	1.029
final R indices [$I > 2\sigma(I)$]	R1 = 0.0616, wR2 = 0.1376
R indices (all data)	R1 = 0.1131, wR2 = 0.1681
largest diff. peak and hole	0.475 and −0.538 e·Å^{-3}

The purities (determined by DSC in the fusion to the liquid crystal phase) were 99.76 (sample A), and 99.43 (sample B). No impurities have been detected by FTIR.

2.2. Single Crystal Preparation. Several attempts were carried out in order to obtain a good single crystal of copper(II) decanoate. For crystal growth, a warm saturated solution of this compound in ethanol, in which both samples A and B were highly soluble, was used. After slow solvent evaporation (during 4−5 weeks) at room temperature, small bluish needles of single crystals (sample C) were obtained. This procedure differs from that of Lomer and Perera[11] (gel diffusion method). One of the needles of appropriate size was studied by single crystal X-ray diffraction, whereas powder X-ray diffraction was carried out on the small needles. DSC, XRD and FTIR experiments, carried out on samples B and C, showed that B and C have exactly the same behavior, and then have the same crystalline structure.

2.3. X-ray Diffraction. (a) Single Crystal X-ray Diffraction. Data collection was carried out at room temperature on a Bruker Smart CCD diffractometer, with graphite-monochromated and Mo Kα radiation (λ = 0.71073 Å), operating at 50 kV and 30 mA. The intensity data were collected over a hemisphere of the reciprocal space by combination of three exposure sets. Each exposure of 20 s covered 0.3° in ω. Reflection range for the data collection was $1.36° < \theta < 27.0°$. The first 100 frames were re-collected at the end of the data collection to monitor crystal decay.

The crystallographic information on polymorph B is summarized in Table 1. The structure was solved by direct methods. The refinement was done by full matrix least-squares procedures on F^2 (SHELXTL version 5.1).[32] All non-hydrogen atoms were refined anisotropically. The hydrogen atoms were calculated at geometrical positions and refined as riding on the respective carbon atoms. Further crystallographic details for the structure reported in this paper may be obtained from the Cambridge Crystallographic Data Center, on quoting the depository number CCDC- 660992.

(b) X-ray Powder Diffraction. Samples were measured at room temperature in reflection mode on a Panalytical X'Pert MPD ALPHA1 diffractometer, equipped with a curved Ge111 primary beam monochromator and a fast detector X'Celerator (Cu Kα1 radiation, 45 kV, 40 mÅ). The measurement range of 2θ was from 3° to 40°, with 101 s/step counting time, and a step size 0.0167°.

For XRD measurements as a function of temperature, a Panalytical X'Pert PRO MPD diffractometer was used. Diffraction patterns were recorded in the range from 3 to 40° 2θ using a detector X'Celerator

Table 2. Description and Correspondence between the Unit Cell Parameters of Lomer's and B Polymorphs, Both Triclinic, Space Group $P\bar{1}$

cell parameters				*d*-spacing description	
Lomer and Perera[a]		sample B[b]		Lomer and Perera[a]	sample B[b]
a/Å	7.94(1)	*c*/Å	16.440(4)	catena lateral packing	breaking direction of catena lateral packing
b/Å	5.28(3)	*a*/Å	5.2035(11)	direction of paddle wheel coordination	direction of paddle wheel coordination
c/Å	28.13(5)	*b*/Å	14.331(3)	bilayer distance direction	interdigitation direction
$\alpha = 94.6(10)°$		$\alpha = 65.390(4)°$			
$\beta = 97.1(5)°$		$\beta = 86.889(4)°$			
$\gamma = 98.6(10)°$		$\gamma = 82.886(4)°$			

[a] Reference.[11b] [b] This work.

(Cu Kα, 45 kV, 40 mÅ) with 50 s/step counting time and a step size of 0.0334°. In situ X-ray powder diffraction measurements up to melt temperature in inert atmosphere (N_2(g)) were done using an Anton Paar HTK-1200 furnace.

2.4. Differential Scanning Calorimetry. A TA Instruments DSC, model Q10 with tightly sealed aluminum volatile pans (in atmosphere of N_2(g)) was used to scan the thermograms at different heating rates (usually at 5 $K \cdot min^{-1}$, again in dry nitrogen atmosphere). An MT5 Mettler microbalance was used to weigh the samples, of about 10 mg (with an error of ±0.001 mg) each. The calorimeter was calibrated in temperature using standard samples of In (purity >99.999% supplied by TA), Sn (>99.9%), and benzoic acid (purity >99.97%, supplied by the former NBS, lot 39i). The standard In and Sn samples already described were used for the enthalpy calibration.

2.5. Optical Microscopy. To identify the nature of the phases (solid, liquid crystal, or liquid), a Carl Zeiss-Jena polarizing optical microscope, model Zeiss Jenalab pol-30-G0527, equipped with a LINKAM hot stage, model THMS600, connected to a LINKAM programmable temperature-controller, model TMS94, was used.

2.6. FTIR Spectroscopy. Infrared spectra of copper(II) decanoate in KBr pellets were recorded using a Nicolet Magna 750 FTIR spectrometer at a resolution of 2 cm^{-1}. A commercial variable temperature cell, SPECAC VTL-2, adapted for solid samples, was employed to obtain IR spectra of the heated salts.

2.7. C-13 NMR Spectroscopy. The solid state C-13 NMR measurements were performed in a Bruker AvanceTM 400 spectrometer (Bruker Analytik GmbH Karlsrube, Germany) equipped with a 89 mm wide bore, 9.4 T superconducting magnet (C-13 Larmor frequency at 100.61 MHz). Powdered samples were placed in 4 mm zirconia rotors. All reported data were acquired at 295 ± 0.1 K with a standard Bruker double resonance 4 mm cross-polarization (CP)/magic angle spinning (MAS) NMR probe head using a 90° C-13 pulse length of 4.2 μs. The C-13 spectra were acquired with 2 ms CP contact time, 5 s recycle delay, MAS spinning rates of 6.5 kHz and 1000 to 4000 transients. High-power proton decoupling of 75 kHz was used. The NMR spectra were evaluated with the spectrometer manufacture's software package XWIN-NMR. All free-induction decays were subjected to standard Fourier transformation with 20 Hz line broadening and phasing. The chemical shifts were externally referenced to adamantane (29.5 ppm) secondary to TMS (0.0 ppm).

3. Results

3.1. X-ray Diffraction. A combination of single-crystal and powder XRD was used to study the polymorph structures.

(a) Single Crystal X-ray Diffraction. The unit cell parameters of the already described Lomer and Perera structure, together with the here reported results for sample B, are shown for comparison in Table 2. Both room temperature crystalline polymorphs belong to the same space group $P\bar{1}$, but differ in the cell parameters and in the packing of the chains. Table 2 also summarizes the description and correspondence of the parameters for both polymorphs. The biggest change observed in polymorph B consists in that the bilayered structure of sample A is lost in sample B, which presents a columnar distribution of the catena inside a net of two-by-two interdigitated chains. Additionally, the correspondence between parameters and their description may help to understand the differences between the polymorphs (Table 2). Figure 2 shows the bilayered and the two by two interdigitated packing of Lomer's and B polymorphs are shown. The angle parameters in the new polymorph B are much less orthogonal than in Lomer's one.

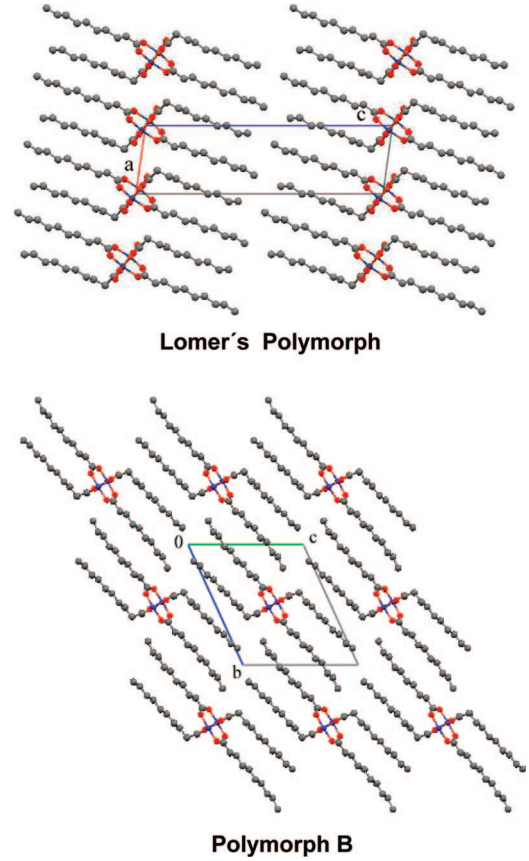

Figure 2. Lomer's polymorph: "*b*" view of the packing showing the lamellar structure. Polymorph B: "*a*" view of the packing showing a columnar distribution and the two by two interdigitated chains. Hydrogen atoms not drawn.

Three views of the unit cell of polymorph B, and the ORTEP plot of paddle wheel molecular unit, with thermal ellipsoids at 50% probability, are shown in Figure 3.

(b) Powder X-ray Diffraction on Crystal Phase of Samples A and B. Powder X-ray patterns were registered on A and B samples, from room temperature to about 140 °C. A combination of single-crystal and powder XRD was used to study their structures. The two CIF files of the Lomer's and B polymorphs were used to simulate the powder XRD pattern. The simulated and the room temperature experimental powder patterns of samples A and B are represented in Figure 4.The simulated and experimental X-ray patterns are exactly the same for polymorph B thus indicating that the single crystal grown in ethanol is the same polymorph recrystallized in benzene. The comparison of the equivalent diffractograms of Lomer's simulated and the room temperature of sample A are very close for

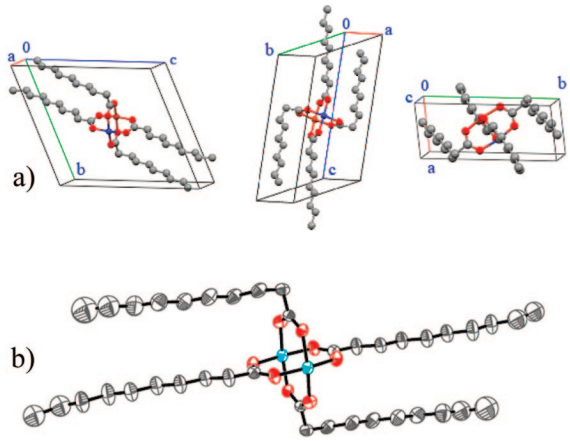

Figure 3. Polymorph B: (a) Different views of the unit cell. (b) ORTEP plot with thermal ellipsoids at 50% probability. Hydrogen atoms not drawn.

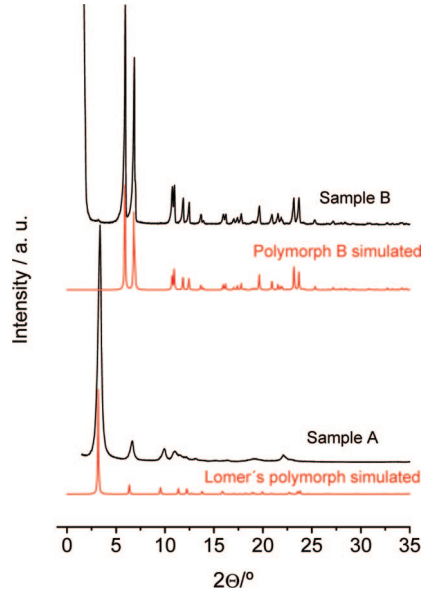

Figure 4. Comparison of the experimental room temperature XRD diffractograms of samples A and B with Lomer's and polymorph B simulated ones.

the first reflections, pointing to a similar structure, but with some disorder (e.g., chain defects) in our sample A.

The simulated diffractograms of both samples were used for indexation of the room temperature diffractograms and helped to determine the (00*l*), (*h*00) and (0*k*0) *d*-spacings as functions of temperature. The sample B spacings were easier to determine because its patterns are better defined than in sample A, pointing again to a more disordered structure in the latter, as shown by C-13 MAS NMR. Figure 5 shows the *d*-spacings and the first heating DSC traces vs temperature for both samples using the same temperature scale.

Spacings corresponding to the direction of the copper(II) coordination between the paddle wheels (through the catena) (d_{0k0} in sample A and d_{h00} in sample B) remain constant in both solids, while the spacing corresponding to the interlayer distance in A (d_{00l}) is about twice the interdigitated spacing in B (d_{0k0}). The lateral packing of coordinated paddle wheels (d_{h00} in sample A) disappears in sample B, due to the interdigitation of the chains, that separates the catena one to another, so the d_{00l} spacing value in B is much higher. On the other hand, in sample A, small fluctuations in all of the *d*-spacings were measured at temperatures corresponding to the exo−endo effect (premelting) observed by DSC. Powder X-ray patterns registered on sample C (single crystals grown in ethanol) were exactly the same as that shown for sample B in Figure 4, confirming, as it was said before, the same structure of both samples.

(c) X-ray Diffraction on Liquid Crystal Phase. Diffractograms taken on the liquid crystal phase of both samples were identical and very simple, showing only three sharp Bragg reflections of the same series, from which only one *d*-spacing was obtained for this phase. This simplicity can be attributed to fluctuations in the interlayer distances, taking place in these organized fluid phases (between columns in its hexagonal array).[33] The *d*-spacing was evaluated and fits perfectly in the plot of *d*-spacing vs number of carbons reported by Ibn-Elhaj et al.[4] for this mesomorphic phase; as it was already mentioned, copper(II) decanoate was not included in this report. The slope of this plot corresponds to the size occupied by two CH_2 groups statiscally oriented in melted chains, at this temperature. In Figure 6, a schematic representation of the columnar discotic liquid crystal (CDLC), based in the description of this mesophase made by Donnio,[15] is shown.

The *d*-spacing of samples A and B in the CDLC phase has the same value, and slightly increases with temperature (from 15.6 Å up to at 15.8 Å) at the lowest and the highest temperature, respectively (see Figure 5, to the right). This confirms the same nature of the liquid crystal for both samples.

(d) Thermal Coefficients. As it was said, explained above, the simulated powder diffractograms of Lomer and polymorph B were used for indexation of lines of the powder X-ray patterns at room temperature. Thanks to this indexation, the evolution of the Bragg reflection could be followed and the d_{00l}, d_{0k0} and d_{h00}, for A and B samples as functions of temperature, were thus evaluated. The corresponding *d*-spacing ratios vs temperature are shown in Figure 7. In this figure, the evolution of the three linear thermal coefficients (α) along the principal axes (the slope of the lines) can be followed. For sample A, these coefficients show a jump at the temperature of the exo−endo effect, associated with a transition from the triclinic solid to the hexagonal structure of the CDLC mesomorph, and vary almost linearly in the range 25 and 70 °C. These values are $\alpha_a = 3.4(9) \times 10^{-4}\ K^{-1}$, $\alpha_b = 9.8(1) \times 10^{-4}\ K^{-1}$, $\alpha_c = -2.2(6) \times 10^{-4}\ K^{-1}$. The thermal coefficient corresponding to the interlamellar d_{00l} spacing is negative in this sample, which must be due to formation of chain defects. On the contrary, for sample B, these coefficients are temperature independent and their values are positive: $\alpha_a = 6.7(6) \times 10^{-4}\ K^{-1}$, $\alpha_b = 4.1(7) \times 10^{-4}\ K^{-1}$, $\alpha_c = 5.3(7) \times 10^{-4}\ K^{-1}$. This fact reflects that in polymorph A the alkyl chains are freer to move than in the interdigitated form B.

(e) Polytypism or Monotropic Polymorphism. The nature of A and B polymorphs is monotropic because the conversion of one into another never appeared in the same thermogram. The generally accepted definition of polytypism implies "a special case of polymorphism in which the various polymorphs (polytypes) are derived from the different ways of stacking structurally identical layers".[34,35] Our two polymorphs do not fit this definition, because although both crystallize in the same crystallographic system and belong to the same group of symmetry, one is bilayered and the other one columnar. Thus, polytypism should be then ruled out.

On the other hand, Herbstein[29] defined polymorphism as "the occurrence of different crystal structures for the same chemical entity. The *n* phase of a one-component system is enantiotropic

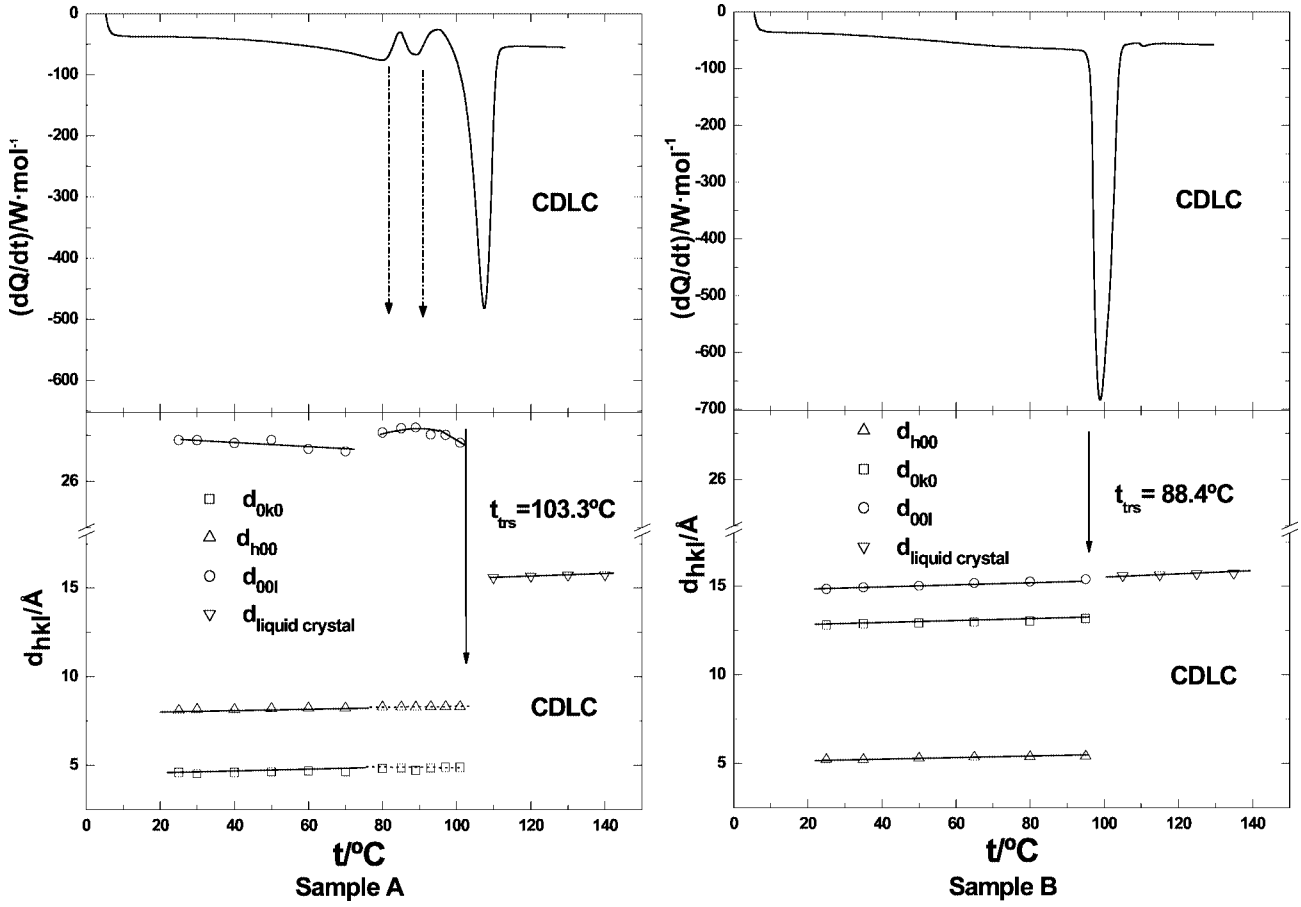

Figure 5. DSC thermograms and *d*-spacings vs temperature, for samples A (recrystallized in *n*-heptane) and B (recrystallized in benzene); CDLC = columnar discotic liquid crystal.

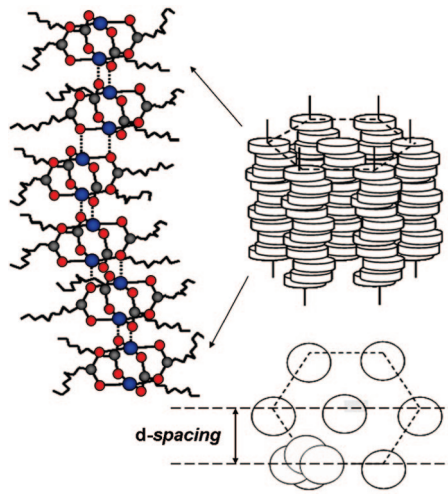

Figure 6. Schematic representation of the hexagonal CDLC phase for the copper(II) decanoate. *d*-spacing measured would correspond with the apothem of the hexagonal section.

if there are (n − 1) phase transformations below the melting point, but monotropic if there are no such transformations (at atmospheric pressure)". This definition seems to be valid yet and within the considerations written in the introductory article to the special issue on *Polymorphism in Crystals* by Desiraju.[30] Thus, it would be more appropriate to describe the behavior found for the copper(II) decanoate as monotropic polymorphism.

3.2. DSC. A summary of the thermal behavior of copper(II) decanoate is shown in Figure 8 for the different samples described in section 2.1, registered at a heating rate of 5 °C·min^{-1}.

Figure 8I shows the thermogram obtained for the first heating of sample A. An exo−endo effect appears at about 80 °C, and ending before the fusion at 102.3 ± 0.5 °C. $\Delta_{fus}H$ and $\Delta_{fus}S$ are (27.4 ± 0.6) kJ·mol^{-1}, and (73 ± 1) J·mol^{-1}·K^{-1}, respectively. The values were measured by extrapolating the upper baseline of the thermogram and are clearly underestimated because of this exo−endo thermal effect. The thermogram also describes the thermal behavior of both samples (previously melted and cooled at room temperature) after waiting for several days at room temperature.

The thermogram of sample B on its first heating is shown in Figure 8II. Only a peak of fusion appears, at a lower temperature than that of sample A. Temperature of fusion, $\Delta_{fus}H$ and $\Delta_{fus}S$ are (96.4 ± 0.5) K, (38.2 ± 0.8) kJ·mol^{-1}, and (103 ± 2) J·mol^{-1}·K^{-1}, respectively. Figures 8III and 8IV show the second thermograms on heating, of samples A and B, both registered immediately after being cooled, respectively. Both samples A and B melt to the same liquid crystal phase, which decomposes at about 260 °C, before reaching the clearing point.

A DSC study was also done on sample C (single crystals in ethanol), but results were exactly the same as shown for sample B.

Samples A and B correspond to two polymorphs. Sample A should be the thermally stable phase because the higher melting point and presumably higher enthalpy of fusion. Since a

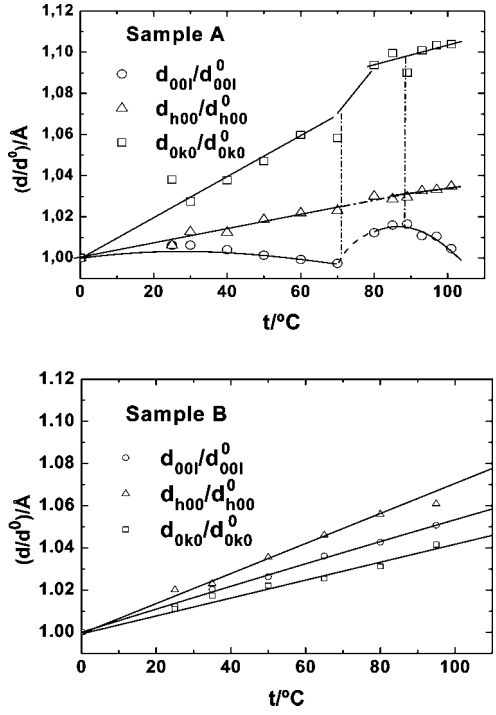

Figure 7. Unit cell parameter ratio vs temperature, for samples A and B. Slopes represent the thermal expansion coefficients along the specified axis.

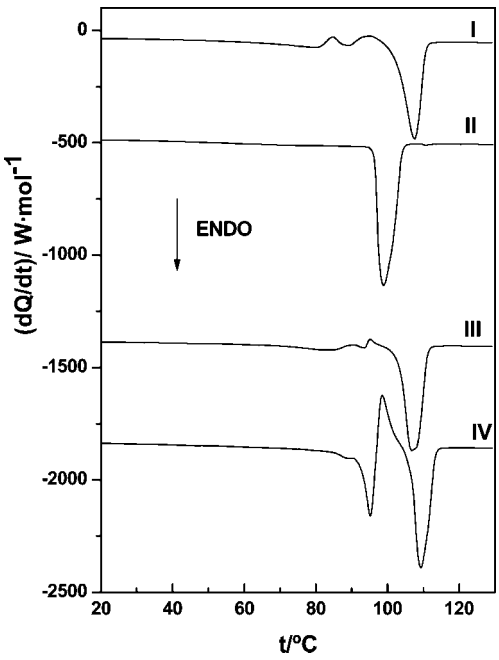

Figure 8. DSC thermograms, registered at 5 °C·min^{-1}. I: Sample A, first heating, and also second and next heatings of samples A and B, after waiting for several days. II: Sample B, first heating. III and IV: Second heatings of samples A and B, respectively, registered immediately after being cooled.

transition from phase A to B was not found in any of the thermogram, the polymorphism is monotropic.

3.3. Optical Microscopy. Observation of textures upon cooling the isotropic melts was not possible because this compound decomposes before reaching the clearing point, at several degrees above the first fusion to liquid crystal. The technique suggested by Demus and Richter[36] (evaporating the solvent at a liquid crystal phase temperature of a solution of the sample) was adopted to carry out visual observations of the mesophases with the microscope. Only a birefringent fluid phase (without any texture) was observed as a proof of the liquid crystal phase. In addition, we used a second and definitive method, consisting in the observation of salt with small amounts of the corresponding acid mixture. We observed developable domains of the pure copper(II) decanoate (see Figure 9) in its mesomorphic state, and could identify then as an hexagonal columnar discotic liquid crystal,[37] in agreement with other authors,[38] that had carried out X-ray diffraction in this phase.

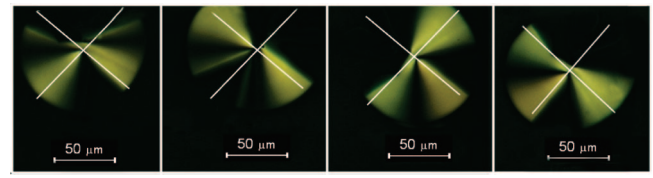

Figure 9. Typical developable domains of the hexagonal columnar discotic liquid crystal observed by optical microscopy. Cross polars fixed, and sample rotated 90° each time.

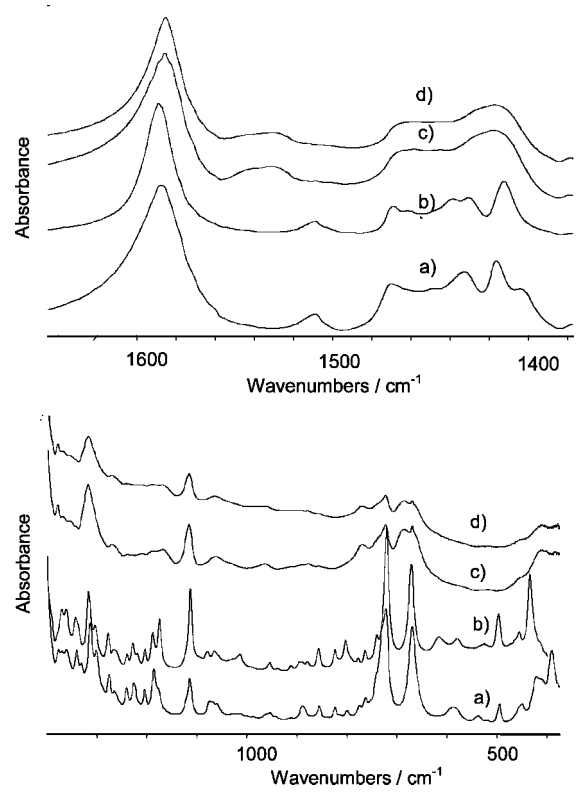

Figure 10. FTIR spectra of copper(II) decanoate of (a) polymorph A and (b) polymorph B, at room temperature, and (c and d) after fusion.

3.4. FTIR Spectroscopy. Figure 10 shows the FTIR spectra of the two polymorphs of copper(II) decanoate at room temperature and after their fusion. Although the spectra of the two samples are very similar, a detailed study of the spectra allows recognition of the characteristic features of each polymorph. Differences are observed in the frequency corresponding to the carboxylate asymmetric stretching (1588 cm^{-1} and 1585 cm^{-1} for polymorphs A and B respectively) and symmetric stretching bands (two bands at 1416 and 1406 cm^{-1} in polymorph A, one band at 1412 cm^{-1} in B). The separation between the ν_{asym} and ν_{sym} wavenumbers ($\Delta\nu \cong 170$ cm^{-1} in both samples) is in agreement with a bridging bidentate

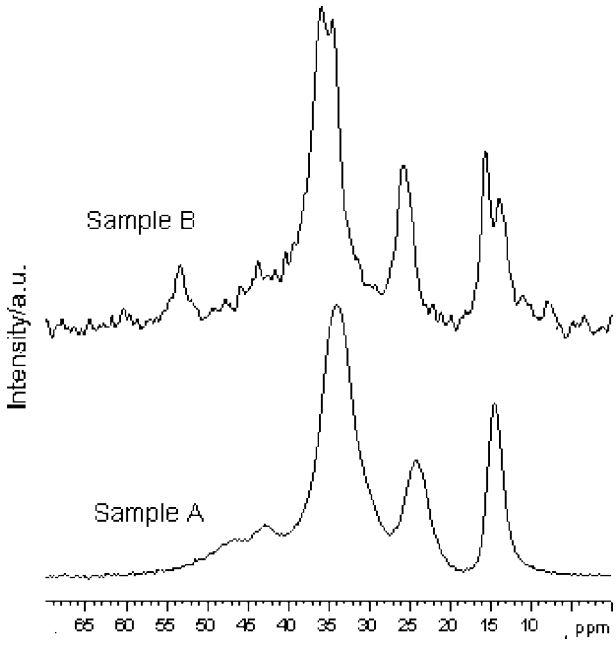

Figure 11. C-13 MAS NMR spectra of copper(II) decanoate for both samples, at 295 K.

coordination of the carboxylate group.[39] In addition, we also observe differences in the bands assigned to the CH_3 symmetric bending (umbrella mode) with a band at 1377 cm^{-1} in solid A that does not appear in solid B, and in the CH_3 rocking vibration around 890 cm^{-1} (three bands in B and only two in A). All these features must be ascribed to two different solid structures (interpenetrating chains in solid B and with lamellar chains in solid A), as observed by other techniques. In addition, the frequencies of Cu−O stretching, bands below 450 cm^{-1}, are different in the two solids and could correspond to the dissimilar Cu−O distances measured by X-ray data single crystal. Besides, bands ascribed to COO^- wagging vibration differ in the two solids: a single band at 587 cm^{-1} is present in sample A at the low temperature spectrum, whereas two bands at 579 and 617 cm^{-1} are observed in the spectrum of sample B. According to Zerbi et al.,[40] this mode frequency is very sensitive to the conformation of the alkyl chain with respect to the carboxylate group. Our X-ray data show that the only significant difference in the carboxylate environment is the proximity of the methyl end chain in B due to the interdigitated chain structure.

After fusion, both solids have the same structure and their spectra are identical (Figure 10, c and d), which is in agreement with the DSC and X-ray results. The measured value of $\Delta\nu$ between the asymmetric and symmetric carboxylate stretching bands remains at around 170 cm^{-1}, thus indicating that the bridging bidentate coordination is also present in the mesophase, in disagreement with some authors.[7]

3.5. C-13 NMR Spectroscopy. Figure 11 illustrates the C-13 MAS NMR spectra of copper(II) decanoate corresponding to (bottom) sample A and (top) sample B, at 295 K. Five groups of signals corresponding to the methyl and methylene carbon atoms in the compound are observed.[41] Due to the line broadening effect induced by the nearby paramagnetic Cu^{2+} ions no peaks corresponding to carboxylic carbons are visible at the resonance frequency. Overall, the spectrum of sample A exhibits broader lines than the spectrum of sample B, which is indicative of a higher molecular order (in aliphatic chains) in the latter. The resonance attributed to the methyl group (14.5 ppm) appears split in the spectrum of sample B, suggesting the presence of two types of environments for the methyl group in this sample. Also, the peak of carbons in α-position shows a displacement toward lower field (from 42.9 to 53.3 ppm) due, most likely, to an electronic unshielding of their nuclei caused by the carboxyl and Cu^{2+}. All of this is in agreement with results obtained by other techniques.

4. Conclusions

Depending on the solvent used for crystallization, two polymorphs of copper(II) decanoate were observed. One of the polymorphs (sample A, recrystallized in pure *n*-heptane) was identified by powder X-ray diffraction and found to be similar to that previously reported in the literature at room temperature.[11b] An X-ray diffraction study performed on a single crystal obtained by growth in ethanol solution showed a different polymorph (sample B). The latter phase was identified as the metastable form by means of calorimetry, that is, its melting point and enthalpy of fusion were lower than those of the stable form. The room temperature crystals of both polymorphs belong to the same space group, $P\bar{1}$, but differ in the unit cell parameters. The biggest difference observed is in the parameter *c* of polymorph A, which diminishes until the half of its corresponding parameter *b* of polymorph B (corresponding to the interdigitated chain direction). Although the cell volumes (1106.01 $Å^3$ and 1151.23 $Å^3$, for polytype B and Lomer's[11b] one, respectively) are roughly the same, there is another important structural difference: the stable form is bilayered, alternating lipidic (end-to-end of the $-CH_3$ groups of the chain) and molecular complexes (paddle wheels). On the other hand, the molecular complexes in the metastable polymorph are stacked in columns within the triclinic structure, and separated by an organized net of two by two interdigitated chains. This arrangement can be appreciated in Figure 2, where the *c* projections and the *a*−*b* face are drawn. Both polymorphs melt to a same columnar discotic liquid crystal phase (as identified by optical microscopy), that decomposes before reaching the clearing point.

Additionally, the structure of sample B is much closer to the hexagonal columnar discotic liquid crystal than that of sample A. The exo−endo effect observed in this sample can explained as a premelting effect in which the chains have to break their lateral packing and conformational order with formation of conformational defects to get the "melted chains" surrounding the coordinated paddle wheel columns in the discotic liquid crystal phase.

An X-ray crystallographic information file (CIF) is available for the novel polymorph at the Cambridge Crystallographic Data Centre, on quoting the depository number CCDC- 660992.

Acknowledgment. Partial support of this research by the Grupo Santander-Universidad Complutense is greatly acknowledged (Project PR41/06-1498). We also thank Dr. E. Matesanz, of the CAI of "Difracción de rayos X" (Universidad Complutense), for his help during the powder XRD experiments. Authors also acknowledge the "CAI de Espectroscopía" (Universidad Complutense) for the use of their facilities.

References

(1) (a) Abied, H.; Guillon, D.; Skoulios, A.; Weber, P.; Giroud-Godquin, A. M.; Marchon, J. C. *Liq. Cryst.* **1987**, *2*, 269–279. (This article was reedited: *Liq. Cryst.* **2006**, *33* (11−12), 1249−1254). (b) Maldivi, P.; Guillon, D.; Giroud-Godquin, A. M.; Marchon, J. C.; Abied, H.; Dexpert, H. A.; Skoulios, A. *J. Chim. Phys.* **1989**, *86*, 1651–1654. (c) Ibn-Elhaj, M.; Guillon, D.; Skoulios, A.; Giroud-Godquin, A. M.; Maldivi, P. *Liq. Cryst.* **1992**, *11* (5), 731–744.

(2) Giroud-Godquin, A. M.; Marchon, J. C.; Guillon, D.; Skoulios, A. *J. Phys. Lett. (Paris)* **1984**, *45* (13), L681–L684.
(3) Giroud-Godquin, A. M.; Maldivi, P.; Marchon, J. C.; Aldebert, P.; Peguy, A.; Guillon, D.; Skoulios, A. *J. Phys. (Paris)* **1989**, *50* (5), 513–519.
(4) Ibn-Elhaj, M.; Guillon, D.; Skoulios, A.; Giroud, Godquin.; Marchon, J. C. *J. Phys. II Fr.* **1992**, *2*, 2197–2206.
(5) Barr, M. R. *Can. J. Anal. Sci. Spectrosc.* **1997**, *42*, 121–129.
(6) (a) García, M. V.; Redondo, M. I.; González Tejera, M. J.; Cheda, J. A. R. *Spectrochim. Acta* **1995**, *51A* (3), 341–347. (b) Cheda, J. A. R.; García, M. V.; Redondo, M. I.; Gargani, S.; Ferloni, P. *Liq. Cryst.* **2004**, *31* (1), 1–14.
(7) (a) Ramos Moita, M. F.; Duarte, M. L. T. S.; Fausto, R. *J. Chem. Soc., Faraday Trans.* **1994**, *90* (19), 2953–2960. (b) Fausto, R.; Ramos Moita, M. F.; Duarte, M. L. T. S. *J. Mol. Struct.* **1995**, *349*, 439–442.
(8) Strommen, D. P.; Giroud-Godquin, A. M.; Maldivi, P.; Marchon, J. C. *Liq. Cryst* **1987**, *2* (5), 689–699.
(9) Abied, H.; Guillon, D.; Skoulios, A.; Giroud-Godquin, A. M.; Marchon, J. C. *Colloid Polym. Sci.* **1988**, *266*, 579–582.
(10) Fausto, R.; Duarte, M. L. T. S.; Ramos Moita, M. F.; Frunza, L.; Beiça, T.; Frunza, S. *J. Therm. Anal.* **1998**, *52*, 133–139.
(11) (a) Bird, M. J.; Lomer, T. R. *Acta Crystallogr. B* **1972**, *28*, 242–246. (b) Lomer, T. R.; Perera, K. *Acta Crystallogr. B* **1974**, *30*, 2912–2913. (c) Lomer, T. R.; Perera, K. *Acta Crystallogr. B* **1974**, *30*, 2913–2915.
(12) Ghermani, N.; Lecomte, C.; Rapin, C.; Stirmetz, T.; Steimmetz, J.; Malaman, B. *Acta Crystallogr. B* **1994**, *50*, 157–160.
(13) Corbell, M. C.; Robinet, L. *Powder Diffr.* **2002**, *17* (1), 52–69.
(14) Giroud-Godquin, A. M. *Coord. Chem. Rev.* **1998**, *178*−*180*, 1485–1499.
(15) Donnio, B. *Curr. Opin. Colloid Interface Sci.* **2002**, *7*, 371–394.
(16) Mrozinski, J. *Coord. Chem. Rev.* **2005**, *249*, 2534–2548.
(17) Kato, M.; Muto, Y. *Coord. Chem. Rev.* **1988**, *92*, 45–83.
(18) Doyle, A.; Felcman, J.; Gambardella, M. T. P.; Verani, C. N.; Tristao, M. L. B. *Polyhedron* **2000**, *19*, 2621–2627.
(19) Kozlevcar, B.; Leban, I.; Petric, M.; Petricek, S.; Roubeau, O.; Reedijk, J.; Segedin, P. *Inorg. Chim. Acta* **2004**, *357*, 4220–4230.
(20) Vaughan, G. B. M.; Schmidt, S.; Poulsen, H. F. *Z. Kristallogr.* **2004**, *219*, 813–825.
(21) Battaglia, L. P.; Corradi, A. B.; Menabue, L. *J. Chem. Soc., Dalton Trans.* **1986**, *8*, 1653–1657.
(22) Goto, M.; Kani, Y.; Tsuchimoto, H. T.; Ohba, S.; Matsushima, H.; Tokii, T. *Acta Crystallogr. C* **2000**, *56*, 7–11.
(23) Jašková, J.; Mikloš, D.; Korabik, M.; Jorík, V.; Segl'a, P.; Kaliňáková, B.; Hudecová, D.; Švorec, J.; Fischer, A.; Mrozinski, J.; Lis, T.; Melník, M. *Inorg. Chim. Acta* **2007**, *360*, 2711–2720.
(24) Mrozinski, J.; Heyduk, E.; Korabik, M. *Bull. Pol. Acad. Chem.* **1994**, *42* (2), 169–180.
(25) Papaefstathiou, G. S.; MacGillivray, L. R. *Coord. Chem. Rev.* **2003**, *246*, 169–184.
(26) Mao, G.; Dong, W.; Kurth, D. G.; Möhwald, H. *Nano Lett.* **2004**, *4*, 249–252.
(27) Kim, Y. H.; Kan, Y. S.; Jo, B. G.; Jeong, J. H. *Mol. Cryst. Liq. Cryst.* **2006**, *445*, 231–238.
(28) Nasibulin, A. G.; Kauppinen, E. I.; Brown, D. P.; Jokiniemi, J. K. *J. Phys. Chem. B* **2001**, *105*, 11067–11075.
(29) Herbstein, F. H. *Cryst. Growth Des.* **2004**, *4* (6), 1419–1429.
(30) Desiraju, G. R. *Cryst. Growth Des.* **2008**, *8* (1), 3–5.
(31) Yoder, C. H.; Smith, W. D.; Katolik, V. L.; Hess, K. R.; Thomsen, M. W.; Yoder, C. S.; Bullock, E. R. *J. Chem. Educ.* **1995**, *72*, 267–269.
(32) Sheldrick, G. M. *SHELX97, Program for Refinement of Crystal Structure*; University of Göttingen: Göttingen, Germany, 1997.
(33) (a) Busico, V.; Cernichiaro, P.; Corradini, P.; Vacatello, M. *J. Phys. Chem* **1983**, *87*, 1631–1635. (b) Busico, V.; Ferraro, A.; Vacatello, M. *J. Phys. Chem* **1984**, *88*, 4055–4058.
(34) Angel, R. J. *Z. Kristallogr.* **1986**, *176*, 193–204.
(35) Trigunayat, G. C. *Solid State Ionics* **1991**, *48*, 3–70.
(36) Demus, D.; Richter, L. *Textures of Liquid Crystals*; Verlag Chemie: Berlin, 1978; p 92.
(37) Chandrasekhar, S.; Ranganath, G. S. *Rep. Prog. Phys.* **1990**, *53*, 57–84.
(38) Abied, H.; Guillon, D.; Skoulios, A.; Dexpert, A.; Giroud-Godquin, A. M.; Marchon, J. C. *J. Phys. (Paris)* **1988**, *49*, 345–352.
(39) Nakamoto, K. In *Infrared and Raman spectra of Inorganic and Coordination Compounds. Part III: Coordination Compounds*; John Wiley and Sons: New York, 1986; pp 231−233.
(40) Zerbi, G.; Minomi, G.; Tuloch, A. P. *J. Chem. Phys.* **1983**, *78* (10), 5853–5862.
(41) (a) Campbell, G. C.; Haw, J. F. *Inorg. Chem.* **1988**, *27*, 3706–3709. (b) Campbell, G. C.; Reibenspies, J. H.; Haw, J. F. *Inorg. Chem.* **1991**, *30*, 171–176.

CG800196S